Hybrid Zero Dynamics of Planar Biped Walkers

E.R. Westervelt[*], J.W. Grizzle[+], D.E. Koditschek[†]

Abstract— **Planar, underactuated, biped walkers form an important domain of applications for hybrid dynamical systems. This paper presents the design of exponentially stable walking controllers for general planar bipedal systems that have one degree of freedom greater than the number of available actuators. The within-step control action creates an attracting invariant set—a two dimensional zero dynamics submanifold of the full hybrid model—whose restriction dynamics admits a scalar LTI return map. Exponentially stable periodic orbits of the zero dynamics correspond to exponentially stabilizable orbits of the full model. A convenient parameterization of the hybrid zero dynamics is imposed through the choice of a class of output functions. Parameter optimization is used to tune the hybrid zero dynamics in order to achieve closed-loop, exponentially stable walking with low energy consumption, while meeting natural kinematic and dynamic constraints. The general theory developed in the paper is illustrated on a five link walker, consisting of a torso and two legs with knees.**

Keywords. Bipeds, hybrid systems, zero dynamics, underactuated system, Poincaré sections

I. Introduction

A PLANAR biped walker is a robot that locomotes via alternation of two legs in the sagittal plane (see Figure 1). The models for such robots are necessarily hybrid, consisting of ordinary differential equations to describe the motion of the robot when only one leg is in contact with the ground (single support or swing phase of the walking motion), and a discrete map to model the impact when the second leg touches the ground [30] (double support phase). The complexity of controlling such a system is a function of the number of degrees of freedom of the model as well as the degree of actuation or, more precisely, *underactuation* of the system.

For planar, biped walkers with a torso and *one degree of underactuation*, it was shown for the first time in [24] for a 3-link model, and in [45] for a 5-link model, that these systems admit control designs with provable stability properties. The control designs involved the judicious choice of a set of holonomic constraints that were asymptotically imposed on the robot via feedback control. This was accomplished by interpreting the constraints as output functions, and then combining ideas from computed torque and finite-time stabilization. The latter property was used to reduce the stability analysis of the resulting walking motions to the computation and analysis of a one dimensional Poincaré map. In these control designs, it was observed that various

parameters appearing in the holonomic constraints would affect the walking speed, the torques required to achieve walking, etc., but no systematic method for adjusting the parameters was presented.

This paper introduces an important improvement on the previous design methodology by affording a common framework for stability analysis and performance enhancement. The framework provides systematic design of feedback controllers that achieve exponentially stable walking motions in N-link, one degree of underactuation, planar biped models, while affording adjustment of additional figures of merit—for example, energy consumption—as well. Specifically, a within-step controller is devised whose closed loop incorporates a two dimensional submanifold—the zero set of an appropriately parameterized output map—that is an attracting invariant set with respect to the full hybrid model. The selection of this zero dynamics through the choice of output map parameters affords the choice of practicable kinematic, torque, and power ranges, all while respecting the guarantee of an exponentially stable step.

In the broader spectrum of dynamically dexterous machines, this work builds on the ideas of Koditschek et al. [11,37,41,49] where the goal is not to prescribe the dynamics of systems via reference trajectories, as is often done in the control of legged locomotion (see [15,29,34,35,48] for example) but rather to encode the dynamic task via a lower dimensional target, itself represented by a set of differential equations. Given the demonstrated appearance of internal dynamical models in the animal nervous system [36], and the emerging evidence that these models incorporate a state-event based (as opposed to explicit time-based) representations of the plant [18], it seems plausible to hypothesize that task encoding via internal target dynamics may also play a significant role in animal motor control [21]. Previous work on legged locomotion has touched on this concept without clearly articulating or exploiting its full potential. Sano and Furusho [56] regulated angular momentum as a means of inducing locomotion; Goswami et al. [22] regulated total energy; and Kajita and Tani [34] approximated the robot as an inverted pendulum, regulating its center of mass. Ono et al. [43] slave the control to one of the states of the system, instead of time (see also [44] where this idea is applied to the acrobot). Pratt et al. [46,47] achieved a reduction in complexity through a proposed set of walking principles, such as maintaining the torso at a constant angle and the hips at a constant height above the ground while moving one foot in front of the other. Although in that work, the "target" is first order (gradient) dynamics, the leg transitions are imposed by event driven logic, and it is unclear over what range of initial conditions and perturbations the physical second order hybrid closed loop system may ultimately succeed in maintaining a stable gait. In all such approaches, mechanisms comparable to those developed here impose kinematic or dynamic constraints, enforcing, over the Lagrangian (i.e., away from

[*]**Corresponding author.** Control Systems Laboratory, Electrical Engineering and Computer Science Department, University of Michigan, Ann Arbor, MI 48109-2122, USA, westervelt@ieee.org, 734-936-2830 (office), 734-763-1260 (fax)

[+]Control Systems Laboratory, Electrical Engineering and Computer Science Department, University of Michigan, Ann Arbor, MI 48109-2122, USA, grizzle@umich.edu, 734-763-3598 (office), 734-763-8041 (fax)

[†]Artificial Intelligence Laboratory, Electrical Engineering and Computer Science Department, University of Michigan, Ann Arbor, MI 48109-2110, USA, kod@umich.edu, 734-764-4307 (office), 734-763-1260 (fax)

impact conditions) portion of the state space, low dimensional attracting submanifolds. Here, in contrast, as in [11, 41, 49], the attracting submanifold is also designed to be an invariant set of the Lagrangian portion of the closed-loop system whose restriction dynamics (the zero dynamics in this paper) emerges from the robot's motion itself. However, unlike any previous work, in the present paper, the full hybrid zero dynamics (i.e., the entire reduced order motion of the mechanism including both the Lagrangian and the impact portions) is rendered invariant. In this sense, our present results combine the analytical machinery developed in [24, 45] with the notion of a dynamically targeted postural prescription [41, 57] to provide the first rigorous methodology for a lower-dimensional hybrid target dynamics. Note that [60] can be interpreted as providing a similar result for fully actuated systems and a target dynamics having the same dimension as the system being controlled.

The notion of hybrid zero dynamics is an extension of the notion of zero dynamics for systems described by ordinary differential equations. While the zero dynamics for a system modeled by ordinary differential equations is a well known [31] and increasingly used concept, [5, 33, 51, 59], the hybrid zero dynamics is a novel notion developed in this paper to deal with the impact map that is common in legged locomotion models. The hybrid zero dynamics may be defined analogously to the zero dynamics: the largest internal dynamics compatible with the output being identically zero. The central concern of the paper is to establish a constructive approach to the definition of *hybrid* zero dynamics resulting in useful controllers for robotic walking. The zero dynamics of the swing phase portion of the model have been previously studied in [39] in the context of trajectory planning and tracking for an underactuated biped.

The paper is structured as follows. Section II delineates the class of robot models treated here, in particular, subsuming those introduced in [24, 45]. Section III first develops the zero dynamics of the swing phase of the model [24, 39] using general results in [31]. This establishes a foundation for defining the zero dynamics of a hybrid dynamical system along with a general statement of existence conditions.

In Section IV it is demonstrated that the Poincaré map associated with the hybrid zero dynamics is diffeomorphic to a scalar, LTI system. This renders the stability properties of the zero dynamics transparent. A means for computing the exact upper and lower bounds of the domain of definition of the Poincaré map is also given. The section is closed with a summary of the feedback methodology of [24] which is shown to take exponentially stable orbits of the hybrid zero dynamics to exponentially stable orbits of the full model.

Section V addresses issues associated with computing the hybrid zero dynamics in closed form so that they may be effectively exploited for design via parameter optimization. This is accomplished by specializing to a class of outputs defined by a linear function of the state plus a nonlinear function of a scalar variable. The nonlinear function is further specialized to Bézier polynomials [6], which provide a very convenient parameterization for imposing a variety of constraints associated with the existence of the hybrid zero

dynamics and the periodicity of desired walking motions, among others.

In Section VI a framework for the creation of exponentially stable fixed points through optimization is given. Optimization allows the shaping of the hybrid zero dynamics while satisfying natural kinematic and dynamic constraints. The result of the optimization process is not an optimal trajectory but rather a provably stable, closed-loop system with satisfied design constraints.

Section VII illustrates the presented framework for stability analysis and performance enhancement on a 5-link biped model which is under construction by the French project *Commande de Robots à Pattes* of the *CNRS - GdR Automatique* [1].

II. Robot Model and Modeling Assumptions

This section introduces the class of biped walking models, the central concern of the paper. The model considered is a planar open kinematic chain connected at a single joint called the "hip", comprising two identical open chains called the "legs" and a third called the "torso". As depicted in Figure 1, intentionally suggestive of a human figure, conditions that guarantee the torso remains free in the air, while the legs alternate in ground contact will be imposed. All motions will be assumed to take place in the sagittal plane and consist of successive phases of *single support* (meaning the stance leg is touching the walking surface and the swing leg is not) and *double support* (the swing leg and the stance leg are both in contact with the walking surface).

The two phases of the walking cycle naturally lead to a mathematical model of the biped consisting of two parts: the differential equations describing the dynamics during the single support phase, and a model of the dynamics of the double support phase. In order to avoid the "stiffness" associated with including a second differential equation to model the rapid evolution of the robot's state at the impact time [10, 38, 54], it will be assumed that the transition from one leg to another takes place in an infinitesimal length of time [20, 58]; this assumption entails the use of a rigid contact model to describe the impulsive nature of the impact of the swing leg with the ground. The rigid contact model effectively collapses the double support phase to an instant in time, and allows a discontinuity in the velocity component of the state, with the configuration remaining continuous. The biped model is thus *hybrid* in nature, consisting of a continuous dynamics and a re-initialization rule at the contact event.

An important source of complexity in a biped system is the degree of actuation of the system, or more precisely, the degree of *underactuation* of the system. It will be assumed that there is no actuation at the end of the stance leg. Thus the system is underactuated during walking, as opposed to fully actuated (a control at each joint and the contact point with the ground).

A complete list of hypotheses assumed for the robot model and the desired walking gaits is now enumerated.

Robot hypotheses: The robot is assumed to be:

RH1) comprised of N rigid links with mass, connected by revolute joints with no closed kinematic chains;

RH2) planar, with motion constrained to the sagittal plane;

RH3) bipedal, with identical legs connected at a common point called the hips;

RH4) actuated at each joint; and

RH5) unactuated at the point of contact between the stance leg and ground.

Gait hypotheses: Conditions on the controller will be imposed and shown to insure that the robot's consequent motion satisfies the following properties consistent with the intuitive notion of a simple walking gait:

GH1) there are alternating phases of single support and double support;

GH2) during the single support phase, the stance leg acts as a pivot joint, that is, throughout the contact, it can be guaranteed that the vertical component of the ground reaction force is positive and that the ratio of the horizontal component to the vertical component does not exceed the coefficient of static friction;

GH3) the double support phase is instantaneous and can be modeled as a rigid contact [30];

GH4) at impact, the swing leg neither slips nor rebounds;

GH5) in steady state, successive phases of single support are symmetric with respect to the two legs;

GH6) walking is from left to right, so that the swing leg starts from behind the stance leg and is placed strictly in front of the stance leg at impact.

RH1 and RH2 imply the robot has $(N + 2)$-degrees of freedom (DOF) (N joint angles plus the Cartesian coordinates of the hips, for example). RH4, RH5 and GH2 imply that when walking the robot has one degree of underactuation, i.e., one less control than DOF. It is worth noting that even if there were actuation between the stance leg end and ground, it would be worthwhile to first design a controller under hypothesis RH5 and then add an outer control loop to exploit the torque available at the ankle in order to improve the convergence rate of walking to a desired average forward walking rate or to enlarge the region of attraction of the inner controller.

A. Swing phase model

Under GH2 the dynamic model of the robot during the swing phase has N-DOF. Let $q := (q_1, \cdots, q_N)'$ be a set of angular coordinates describing the configuration of the robot with world reference frame W. Since only symmetric gaits are of interest here, the same model can be used irrespective of which leg is the stance leg if the coordinates are re-labeled after each phase of double support. Using the method of Lagrange, the model is written in the form

$$D(q)\ddot{q} + C(q, \dot{q})\dot{q} + G(q) = Bu. \qquad (1)$$

In accordance with RH4 and RH5, torques u_i, $i = 1$ to $N-1$ are applied between each connection of two links, *but not between the stance leg and ground*. The model is written in state space form by defining

$$\dot{x} = \begin{bmatrix} \dot{q} \\ D^{-1}(q) \left[-C(q, \dot{q})\dot{q} - G(q) + Bu \right] \end{bmatrix} \qquad (2)$$

$$=: f(x) + g(x)u \qquad (3)$$

where $x := (q', \dot{q}')'$. The state space of the model is taken as $TQ := \{ x := (q', \dot{q}')' \mid q \in \mathcal{Q}, \; \dot{q} \in I\!R^N \}$, where $\mathcal{Q}$ is

a simply-connected, open subset of $[0, 2\pi)^N$ corresponding to physically reasonable configurations of the robot (for example, with the exception of the end of the stance leg, all points of the robot being above the walking surface; one could also impose that the knees are not bent backward, etc.). An alternate approach, not used here, would be to define the admissible states through *viability* constraints [3, 10].

B. Impact model

An impact occurs when the swing leg touches the walking surface, also called the ground. The impact between the swing leg and the ground is modeled as a contact between two rigid bodies. In addition to modeling the change in state of the robot, the impact model accounts for the re-labeling of the robot's coordinates that occurs after each phase of double support. The development of the impact model requires the full $(N + 2)$-DOF of the robot. By adding Cartesian coordinates (p_H^h, p_H^v) to the hips (see Figure 1), the following extended model is easily obtained through the method of Lagrange,

$$D_e(q_e)\ddot{q}_e + C_e(q_e, \dot{q}_e)\dot{q}_e + G_e(q_e) = B_e u + \delta F_{\text{ext}}, \qquad (4)$$

with $q_e := (q_1, q_2, \ldots, q_N, p_H^h, p_H^v)'$ and where δF_{ext} represents the vector of external forces acting on the robot at the contact point. If the stance leg end is in contact with the ground and not slipping, the extended coordinates q_e and their velocities $\dot{q}_e$ are related to q and $\dot{q}$ by

$$q_e = \Upsilon(q) \quad \text{and} \quad \dot{q}_e = \frac{\partial \Upsilon(q)}{\partial q} \dot{q}, \qquad (5)$$

where $\Upsilon(q) := (q', p_H^h(q), p_H^v(q))'$, and $p_H^h(q)$ and $p_H^v(q)$ are the horizontal and vertical positions of the hip, respectively.

Impact model hypotheses: The impact model of [30] is used under the following assumptions:

IH1) the contact of the swing leg with the ground results in no rebound and no slipping of the swing leg;

IH2) at the moment of impact, the stance leg lifts from the ground without interaction;

IH3) the impact is instantaneous;

IH4) the external forces during the impact can be represented by impulses;

IH5) the impulsive forces may result in an instantaneous change in the velocities, but there is no instantaneous change in the configuration; and

IH6) the actuators cannot generate impulses and hence can be ignored during impact.

IH1–IH6 imply total angular momentum is conserved [30]. Following an identical development as in [24], the expression relating the velocity of the robot just before impact, $\dot{q}_e^-$, to the velocity just after (without relabeling), $\dot{q}_e^+$, may be written as

$$\Pi^{-1}(q_e^-) \begin{bmatrix} \dot{q}_e^+ \\ F_2^T \\ F_2^N \end{bmatrix} = \begin{bmatrix} D_e(q_e^-)\dot{q}_e^- \\ 0 \end{bmatrix} \qquad (6)$$

where

$$\Pi(q_e) := \begin{bmatrix} D_e(q_e) & -\left(\dfrac{\partial E(q_e)}{\partial q_e} \right)' \\ \dfrac{\partial E(q_e)}{\partial q_e} & 0 \end{bmatrix}^{-1}, \qquad (7)$$

$E(q_e) = (p_2^h(q_e), p_2^v(q_e))'$ are the Cartesian coordinates of the end of the swing leg (see Figure 1), and F_2^T and F_2^N are the integrals of the tangential and normal contact impulsive forces. The existence of the matrix inverse indicated in (6) and (7) is easily verified. Solving (6) yields

$$\begin{bmatrix} \dot{q}_e^+ \\ F_2^T \\ F_2^N \end{bmatrix} = \Pi(q_e^-) \begin{bmatrix} D_e(q_e^-)\dot{q}_e^- \\ 0 \end{bmatrix}. \qquad (8)$$

The map from $\dot{q}_e^-$ to $\dot{q}_e^+$, that is, the map from velocities just prior to impact to just after impact (without relabeling), is obtained by partitioning $\Pi(q_e^-)$ as

$$\dot{q}_e^+ = \Pi_{11}(q_e^-)D_e(q_e^-)\dot{q}_e^- \qquad (9)$$

$$\begin{bmatrix} F_2^T \\ F_2^N \end{bmatrix} = \Pi_{21}(q_e^-)D_e(q_e^-)\dot{q}_e^-. \qquad (10)$$

Combining (5) with (9) and (10) results in an expression for the velocities of the robot just after impact and the integral of the forces experienced by the end of the swing leg at impact. At impact, it is assumed that the swing leg becomes the new stance leg, so the coordinates must be relabeled. Express the relabeling of the states as a linear, invertible transformation matrix, R. The result of the impact and relabeling of the states is then an expression

$$x^+ = \Delta(x^-) \qquad (11)$$

where $x^+ := (q^+, \dot{q}^+)$ (resp. $x^- := (q^-, \dot{q}^-)$) is state value just after (resp. just before) impact and

$$\Delta(x^-) := \begin{bmatrix} \Delta_q\, q^- \\ \Delta_{\dot{q}}(q^-)\, \dot{q}^- \end{bmatrix} \qquad (12)$$

where $\Delta_q := R$ and $\Delta_{\dot{q}}(q^-) := [R \quad 0]\, \Pi_{11} \circ \Upsilon(q^-)D_e \circ \Upsilon(q^-)\, (\partial \Upsilon(q)/\partial q)|_{q=q^-}$.

C. The Plant Model: a Hybrid Nonlinear Underactuated Control System

The overall biped robot model can be expressed as a nonlinear system with impulse effects [64]

$$\begin{aligned} \dot{x} &= f(x) + g(x)u & x^- \notin S \\ x^+ &= \Delta(x^-) & x^- \in S, \end{aligned} \qquad (13)$$

where,

$$S := \{(q, \dot{q}) \in TQ \mid p_2^v(q) = 0,\ p_2^h(q) > 0\}, \qquad (14)$$

and $x^-(t) := \lim_{\tau \nearrow t} x(\tau)$. The value of $p_2^h(q)$ is taken to be positive so that for $x \in S$ the swing leg end is in front of the stance leg as per GH6. Solutions are taken to be right continuous and must have finite left and right limits at each impact event (see [23] for details).

Informally, a *step* of the robot is a solution of (13) that starts with the robot in double support, ends in double support with the configurations of the legs swapped, and contains only one impact event. This is more precisely defined as follows. Let $\varphi(t, x_0)$ be a maximal solution of the swing phase dynamics (3) with initial condition x_0 at time $t_0 = 0$, and define the *time to impact* function, $T_I : TQ \to I\!R \cup \{\infty\}$, by

$$T_I(x_0) := \begin{cases} \inf\{t \geq 0 \mid \varphi(t, x_0) \in S\} & \text{if } \exists\, t \text{ s.t.} \\ & \qquad \varphi(t, x_0) \in S \\ \infty & \text{otherwise} \end{cases} \qquad (15)$$

Let $x_0 \in S$ be such that $T_I \circ \Delta(x_0) < \infty$. A *step* of the robot is the solution of (13) defined on the half-open interval $[0, T_I \circ \Delta(x_0))$ with initial point x_0. Any point $x_0 \in S$ such that $T_I \circ \Delta(x_0) < \infty$ is said to result in the robot taking a step.

III. THE ZERO DYNAMICS OF WALKING

The method of computed torque or inverse dynamics is ubiquitous in the field of robotics [19, 40, 61]. It consists of defining a set of outputs, equal in number to the inputs, and then designing a feedback controller that asymptotically drives the outputs to zero. The task that the robot is to achieve is encoded into the set of outputs in a such a way that the nulling of the outputs is (asymptotically) equivalent to achieving the task, whether the task be asymptotic convergence to an equilibrium point, a surface, or a time trajectory. For a system modeled by ordinary differential equations (in particular, no impact dynamics), the *maximal internal dynamics* of the system that are *compatible with the output being identically zero* is called the *zero dynamics* [31, 32, 42]. Hence, the method of computed torque, which is asymptotically driving a set of outputs to zero, is indirectly designing a set of zero dynamics for the robot. Since in general the dimension of the zero dynamics is considerably less than the dimension of the model itself, the task to be achieved by the robot has been *implicitly* encoded into a lower dimensional system.

One of the main points of this paper is that this process can be *explicitly* exploited in the design of feedback controllers for walking mechanisms, *even in the presence of impacts*. Section III-A will introduce a class of outputs for which the swing phase zero dynamics can be readily identified and analyzed. Section III-B will derive natural conditions under which the swing phase zero dynamics become compatible with the impact model, thereby leading to the notion of a hybrid zero dynamics for the complete model of the biped.

A. Swing phase zero dynamics

This section identifies the swing phase zero dynamics for a particular class of outputs that have proven useful in constructing feedback controllers for bipedal walkers [24, 45]. Since no impact dynamics are involved, the work here is simply a specialization of the general results in [31] to the model (3). The results summarized here will form the basis for defining a zero dynamics of the complete hybrid model of the planar biped walker, which is the desired object for study.

Note that if an output $y = h(q)$ depends only on the configuration variables, then, due to the second order nature of the robot model, the derivative of the output along solutions of (3) does not depend directly on the inputs. Hence its relative degree is at least two. Differentiating the output

once again computes the accelerations, resulting in

$$\frac{d^2y}{dt^2} =: L_f^2 h(q, \dot{q}) + L_g L_f h(q)u. \tag{16}$$

The matrix $L_g L_f h(q)$ is called the decoupling matrix and depends only on the configuration variables. A consequence of the general results in [31] is that the invertibility of this matrix at a given point assures the existence and uniqueness of the zero dynamics in a neighborhood of that point. With a few extra hypotheses, these properties can be assured on a given open set.

Lemma 1: (Swing phase zero dynamics) Suppose that a smooth function h is selected so that
HH1) h is a function of only the configuration coordinates;
HH2) there exists an open set $\tilde{\mathcal{Q}} \subset \mathcal{Q}$ such that for each point $q \in \tilde{\mathcal{Q}}$, the decoupling matrix $L_g L_f h(q)$ is square and invertible (i.e., the dimension of u equals the dimension of y, and h has vector relative degree $(2, \ldots, 2)'$);
HH3) there exists a smooth real valued function $\theta(q)$ such that $(h(q)', \theta(q))' : \tilde{\mathcal{Q}} \to I\!R^N$ is a diffeomorphism onto its image (see Figure 3 for an example $\theta(q)$);
HH4) there exists at least one point in $\tilde{\mathcal{Q}}$ where h vanishes.
Then,
1. $Z := \{x \in T\tilde{\mathcal{Q}} \mid h(x) = 0, L_f h(x) = 0\}$ is a smooth two dimensional submanifold of TQ; and
2. the feedback control

$$u^*(x) = -(L_g L_f h(x))^{-1} L_f^2 h(x) \tag{17}$$

renders Z invariant under the swing dynamics; that is, for every $z \in Z$, $f_{\text{zero}}(z) := f(z) + g(z)u^*(z) \in T_z Z$.
Z is called the *zero dynamics manifold* and $\dot{z} = f_{\text{zero}}(z)$ is called the *zero dynamics*. □

Lemma 1 follows immediately from general results in [31]; a few of the details are outlined here for later use. From hypotheses HH1 and HH3, $\Phi(q) := [h', \theta(q)]'$ is a valid coordinate transformation on $\tilde{\mathcal{Q}}$, and thus

$$\begin{aligned} \eta_1 &= h(q), & \eta_2 &= L_f h(q, \dot{q}), \\ \xi_1 &= \theta(q), & \xi_2 &= L_f \theta(q, \dot{q}), \end{aligned} \tag{18}$$

is a coordinate transformation on $T\tilde{\mathcal{Q}}$. In these coordinates, the system takes the form

$$\begin{aligned} \dot{\eta}_1 &= \eta_2, & \dot{\eta}_2 &= L_f^2 h + L_g L_f h u, \\ \dot{\xi}_1 &= \xi_2, & \dot{\xi}_2 &= L_f^2 \theta + L_g L_f \theta u, \\ y &= \eta_1 \end{aligned} \tag{19}$$

where $(q, \dot{q})$ is evaluated at

$$q = \Phi^{-1}(\eta_1, \xi_1) \tag{20}$$

$$\dot{q} = \left(\frac{\partial \Phi}{\partial q}\right)^{-1} \begin{bmatrix} \eta_2 \\ \xi_2 \end{bmatrix}. \tag{21}$$

Enforcing $y \equiv 0$ results in $(\eta_1 = h = 0, \eta_2 = L_f h = 0)$, u^* as in (17), and the zero dynamics becoming

$$\begin{aligned} \dot{\xi}_1 &= \xi_2 \\ \dot{\xi}_2 &= L_f^2 \theta + L_g L_f \theta u^*. \end{aligned} \tag{22}$$

While it is useful to know that the zero dynamics can be expressed as a second order system, this form of the equations is very difficult to compute directly due to the need to invert the decoupling matrix. However, this can be avoided. Indeed, since the columns of g in (3) are involutive, by [31], page 222, in a neighborhood of any point where the decoupling matrix is invertible, there exists a smooth scalar function γ such that

$$\begin{aligned} \eta_1 &= h(q), & \eta_2 &= L_f h(q, \dot{q}), \\ \xi_1 &= \theta(q), & \xi_2 &= \gamma(q, \dot{q}), \end{aligned} \tag{23}$$

is a valid coordinate transformation and

$$L_g \gamma = 0. \tag{24}$$

Moreover, by applying the constructive proof of the Frobenius theorem of [31], page 23, in a set of coordinates for the robot such that
RH6) the model is expressed in $N - 1$ *relative* angular coordinates, $(q_1, \cdots, q_{N-1})$, plus one *absolute* angular coordinate, q_N,
one obtains that γ can be explicitly computed to be the last entry of $D(q)\dot{q}$, and hence it can be assumed that $\gamma(q, \dot{q})$ has the form $\gamma_0(q)\dot{q}$; it follows that (23) is a valid coordinate change on all of $T\tilde{\mathcal{Q}}$.

In the coordinates (23), the zero dynamics become

$$\begin{aligned} \dot{\xi}_1 &= L_f \theta \\ \dot{\xi}_2 &= L_f \gamma \end{aligned} \tag{25}$$

where there right hand side is evaluated at

$$q = \Phi^{-1}(0, \xi_1) \tag{26}$$

$$\dot{q} = \begin{bmatrix} \frac{\partial h}{\partial q} \\ \gamma_0 \end{bmatrix}^{-1} \begin{bmatrix} 0 \\ \xi_2 \end{bmatrix}. \tag{27}$$

Theorem 1: (Swing phase zero dynamics form) Under the hypotheses of Lemma 1, $(\xi_1, \xi_2) = (\theta(q), \gamma_0(q)\dot{q})$ is a valid set of coordinates on Z, and in these coordinates the zero dynamics take the form

$$\dot{\xi}_1 = \kappa_1(\xi_1)\xi_2 \tag{28}$$

$$\dot{\xi}_2 = \kappa_2(\xi_1). \tag{29}$$

Moreover, if the model (3) is expressed in coordinates satisfying RH6, the following interpretations can be given for the various functions appearing in the zero dynamics:

$$\xi_1 = \theta|_Z \tag{30}$$

$$\xi_2 = \frac{\partial K}{\partial \dot{q}_N}\bigg|_Z \tag{31}$$

$$\kappa_1(\xi_1) = \frac{\partial \theta}{\partial q} \begin{bmatrix} \frac{\partial h}{\partial q} \\ \gamma_0 \end{bmatrix}^{-1} \begin{bmatrix} 0 \\ 1 \end{bmatrix}\bigg|_Z \tag{32}$$

$$\kappa_2(\xi_1) = -\frac{\partial V}{\partial q_N}\bigg|_Z, \tag{33}$$

where $K(q, \dot{q}) = \frac{1}{2}\dot{q}'D(q)\dot{q}$ is the kinetic energy of the robot, $V(q)$ is its potential energy, and γ_0 is the last row of D, the inertia matrix. □

Proof: The form of (28) is immediate by the form of (25) and (27) since both h and γ_0 are functions of q, and hence when restricted to Z, are functions of ξ_1 only.

Suppose now that the model (3) is expressed in coordinates satisfying RH6. Since the kinetic energy of the robot, $K(q, \dot{q})$, is independent of the choice of world coordinate frame [61, page 140], and since q_N fixes this choice, $K(q, \dot{q})$ is independent of q_N. Since $D := \partial \left[(\partial K/\partial \dot{q})'\right]/\partial \dot{q}$ [61, page 141], it follows that $\partial D/\partial q_N = 0$. Let D_N, C_N, and G_N be the last rows of D, C, and G, respectively. Then $\xi_2 = \gamma_0(q)\,\dot{q}$ is equal to $D_N(q)\,\dot{q}$ [24], and thus is equal to $\partial K/\partial \dot{q}_N$ since $K = \frac{1}{2}\dot{q}'D\dot{q}$. Continuing, $\dot{\xi}_2 := L_f\gamma$ becomes

$$L_f\gamma = \left[\begin{array}{cc} \dot{q}'\dfrac{\partial D'_N}{\partial q} & D_N \end{array}\right]\left[\begin{array}{c} \dot{q} \\ -D^{-1}\left[C\dot{q} + G\right] \end{array}\right] \quad (34)$$

$$= \dot{q}'\frac{\partial D'_N}{\partial q}\,\dot{q} - C_N\dot{q} - G_N. \quad (35)$$

Noting that (see [61, page 142])

$$C_N = \dot{q}'\frac{\partial D'_N}{\partial q} - \frac{1}{2}\,\dot{q}'\frac{\partial D}{\partial q_N}, \quad (36)$$

(35) becomes $L_f\gamma = -G_N = -\partial V/\partial q_N$, which, when evaluated on Z, is a function of ξ_1 only. $\quad\square$

B. Hybrid zero dynamics

The goal of this subsection is to incorporate the impact model into the notion of the *maximal internal dynamics compatible with the output being identically zero*, in order to obtain a zero dynamics of the complete model of the biped walker, (13). Towards this goal, let $y = h(q)$ be an output satisfying the hypotheses of Lemma 1 and suppose there exists a trajectory, $x(t)$, of the hybrid model (13) along which the output is identically zero. If the trajectory contains no impacts with S, then $x(t)$ is a solution of the swing phase dynamics and also of its zero dynamics. If the trajectory does contain impact events, then let (t_0, t_f) be an open interval of time containing exactly one impact at t_e. By definition, on the intervals (t_0, t_e) and (t_e, t_f), $x(t)$ is a solution of the swing phase dynamics and hence also of its zero dynamics, so $x(t) \in Z$; since also by definition of a solution, $x^- := \lim_{t \nearrow t_e} x(t)$ exists, is finite, and lies in S, it follows that $x^- \in S \cap Z$. Moreover, by definition of a solution of (13), $x(t_e) := x^+ := \Delta(x^-)$, from which it follows that $\Delta(x^-) \in Z$. On the other hand, if $\Delta(S \cap Z) \subset Z$, then from solutions of the swing phase zero dynamics it is clearly possible to construct solutions to the complete model of the biped walker along which the output $y = h(q)$ is identically zero. This leads to the following definition.

Definition 1: Let $y = h(q)$ be an output satisfying the hypotheses of Lemma 1, and let Z and $\dot{z} = f_{\text{zero}}(z)$ be the associated zero dynamics manifold and zero dynamics of the swing phase model. Suppose that $S \cap Z$ is a smooth, one-dimensional, embedded submanifold of TQ. If $\Delta(S \cap Z) \subset Z$, then the nonlinear system with impulse effects,

$$\begin{array}{rll} \dot{z} &= f_{\text{zero}}(z) & z^- \notin S \cap Z \\ z^+ &= \Delta(z^-) & z^- \in S \cap Z, \end{array} \quad (37)$$

with $z \in Z$, is the *hybrid zero dynamics* of the model (13). $\triangleleft$

Remark 1: From standard results in [9], $S \cap Z$ will be a smooth one-dimensional embedded submanifold if $S \cap Z \neq \emptyset$ and the map $[h'\ (L_f h)'\ p_2^v{}']'$ has constant rank equal to $2N - 1$ on $S \cap Z$. A simple argument shows that this rank condition is equivalent to rank of $[h'\ p_2^v]' = N$, and under this rank condition, $S \cap Z \cap \tilde{\mathcal{Q}}$ consists of the isolated zeros of $[h'\ p_2^v]'$. Let q_0^- be a solution of $(h(q), p_2^v(q)) = (0, 0)$, $p_2^h(q) > 0$. Then the connected component of $S \cap Z$ containing q_0^- is diffeomorphic to $\mathbb{R}$ per $\sigma : \mathbb{R} \to S \cap Z$, where

$$\sigma(\omega) := \left[\begin{array}{c} \sigma_q \\ \sigma_{\dot{q}}\,\omega \end{array}\right] \quad (38)$$

$\sigma_q := q_0^-$, and

$$\sigma_{\dot{q}} = \left[\begin{array}{c} \frac{\partial h}{\partial q}(q_0^-) \\ \gamma_0(q_0^-) \end{array}\right]^{-1}\left[\begin{array}{c} 0 \\ 1 \end{array}\right]. \quad (39)$$

In view of this, the following additional assumption is made about the output h and the open set $\tilde{\mathcal{Q}}$

HH5) there exists a unique point $q_0^- \in \tilde{\mathcal{Q}}$ such that $(h(q_0^-), p_2^v(q_0^-)) = (0, 0)$, $p_2^h(q_0^-) > 0$ and the rank of $[h'\ p_2^v]'$ at q_0^- equals N.
$\hfill\triangleleft$

The next result characterizes when the swing phase zero dynamics are compatible with the impact model, leading to a non-trivial hybrid zero dynamics.

Theorem 2: (Hybrid zero dynamics existence) Consider the robot model (13) satisfying RH1–RH6 and IH1–IH6 with a smooth function h satisfying HH1–HH5. Then, the following statements are equivalent:
(a) $\Delta(S \cap Z) \subset Z$;
(b) $h \circ \Delta|_{(S \cap Z)} = 0$ and $L_f h \circ \Delta|_{(S \cap Z)} = 0$;
(c) there exists at least one point $(q_0^-, \dot{q}_0^-) \in S \cap Z$ such that $\gamma_0(q_0^-)\,\dot{q}_0^- \neq 0$, $h \circ \Delta_q(q_0^-) = 0$, and $L_f h \circ \Delta(q_0^-, \dot{q}_0^-) = 0$.
$\hfill\square$

Proof: The equivalence of (a) and (b) is immediate from the definition of Z as the zero set of h and $L_f h$. The equivalence of (b) and (c) follows from Remark 1 once it is noted from (12) that $L_f h \circ \Delta$ is linear in $\dot{q}$. $\quad\square$

Under the hypotheses of Theorem 2, the hybrid zero dynamics are well-defined. Let $z^- \in S \cap Z$, and suppose that $T_I \circ \Delta(z^-) < \infty$. Set $z^+ = \Delta(z^-)$ and let $\varphi : [0, t_f] \to Z$, $t_f = T_I(z^+)$, be a solution of the zero dynamics, (22), such that $\varphi(0) = z^+$. Define $\hat{\theta}(t) := \theta \circ \varphi(t)$ and $\dot{\hat{\theta}} := d\hat{\theta}(t)/dt$.

Proposition 1: Assume the hypotheses of Theorem 2. Then over any step of the robot, $\dot{\hat{\theta}} : [0, t_f] \to \mathbb{R}$ is never zero. In particular, $\hat{\theta} : [0, t_f] \to \mathbb{R}$ is strictly monotonic and thus achieves its maximum and minimum values at the end points. $\hfill\square$

The proof is given in the appendix. By Remark 1, it follows that $\hat{\theta}(0) = \theta \circ \Delta_q(q_0^-)$ and $\hat{\theta}(t_f) = \theta(q_0^-)$, that is, the extrema can be computed *a priori*. Denote these by

$$\theta^- := \theta(q_0^-) \quad (40)$$

$$\theta^+ := \theta \circ \Delta_q(q_0^-). \quad (41)$$

Without loss of generality, it is assumed that $\theta^+ < \theta^-$; that is, along any step of the hybrid zero dynamics, θ is *monotonically increasing*.

Remark 2: The fact that θ evaluated along a step of the zero dynamics must be monotonic implies that there are restrictions on the walking gaits that can be achieved through computed-torque control based on an output that depends only on the configuration variables. ◁

IV. STABILITY ANALYSIS OF THE ZERO DYNAMICS

Now, an explicit expression for the Poincaré map of the hybrid zero dynamics will be derived, along with a precise determination of its domain of definition. Fixed points of the Poincaré return map of the hybrid zero dynamics correspond to periodic orbits of the hybrid zero dynamics. When the hybrid zero dynamics admit an exponentially stable periodic orbit, the general feedback approach developed in [24, 45] can be immediately applied to create a provably, exponentially stable periodic orbit in the full hybrid model.

A. Poincaré analysis of the zero dynamics

It is shown here that the Poincaré map associated with (37) is diffeomorphic to a scalar LTI system, reducing determination of the local stability properties of its fixed point to a simple explicit computation.

Assume the hypotheses of Theorem 2. Take the Poincaré section to be $S \cap Z$ so that the Poincaré map is the partial map $\rho : S \cap Z \to S \cap Z$ defined as follows [24]: let $\varphi(t, z_0)$ be a solution of the zero dynamics f_{zero} and consider the time to impact function, (15), restricted to Z. Since both $f_{\text{zero}}(z)$ and Z are smooth, a solution of (28)–(29) from a given initial condition, z_0, is unique and depends smoothly on z_0. Then by [24, Lemma 3], $\tilde{Z} := \{z \in Z \mid 0 < T_I(z) < \infty \text{ and } L_f p_2^v(\varphi(T_I(z), z)) \neq 0\}$ is open. Define the Poincaré return map for the hybrid zero dynamics as

$$\rho(z) := \varphi(T_I \circ \Delta(z), \Delta(z)). \tag{42}$$

In a special set of local coordinates, the return map can be explicitly computed. Indeed, express the hybrid zero dynamics in the coordinates of Theorem 1, namely, $(\xi_1, \xi_2) = (\theta, \gamma)$. In these coordinates, $S \cap Z$ and $\Delta : (\xi_1^-, \xi_2^-) \to (\xi_1^+, \xi_2^+)$ simplify to

$$S \cap Z = \left\{ (\xi_1^-, \xi_2^-) \mid \xi_1^- = \theta^-, \xi_2^- \in \mathbb{R} \right\} \tag{43}$$

$$\xi_1^+ = \theta^+ \tag{44}$$

$$\xi_2^+ = \delta_{\text{zero}} \xi_2^-, \tag{45}$$

where $\delta_{\text{zero}} := \gamma_0(q^+) \, \Delta_{\dot{q}}(q_0^-) \, \sigma_{\dot{q}}(q_0^-)$, a constant that may be computed *a priori*. The hybrid zero dynamics are thus given by (28)–(29) during the swing phase, and at impact with $S \cap Z$, the re-initialization rules (44) and (45) are applied. By Proposition 1, over any step $\dot{\xi}_1$ is non-zero, and thus (28)–(29) are equivalent to

$$\frac{d\xi_2}{d\xi_1} = \frac{\kappa_2(\xi_1)}{\kappa_1(\xi_1)\xi_2}. \tag{46}$$

From (30), $\dot{\xi}_1 \neq 0$ implies $\xi_2 \neq 0$, and thus $\zeta_2 := \frac{1}{2}(\xi_2)^2$ is a valid change of coordinates on (46). In these coordinates, (46) becomes

$$\frac{d\zeta_2}{d\xi_1} = \frac{\kappa_2(\xi_1)}{\kappa_1(\xi_1)}. \tag{47}$$

For $\theta^+ \leq \xi_1 \leq \theta^-$, define[1]

$$V_{\text{zero}}(\xi_1) := -\int_{\theta^+}^{\xi_1} \frac{\kappa_2(\xi)}{\kappa_1(\xi)} \, d\xi \tag{48}$$

$$\zeta_2^- := \frac{1}{2}(\xi_2^-)^2 \tag{49}$$

$$\zeta_2^+ := \delta_{\text{zero}}^2 \, \zeta_2^-. \tag{50}$$

Then (47) may be integrated over a step to obtain

$$\zeta_2^- = \zeta_2^+ - V_{\text{zero}}(\theta^-), \tag{51}$$

as long as[2] $\zeta_2^+ - K > 0$, where,

$$K := \max_{\theta^+ \leq \xi_1 \leq \theta^-} V_{\text{zero}}(\xi_1). \tag{52}$$

Theorem 3: (Poincaré map for hybrid zero dynamics) Assume the hypotheses of Theorem 2 and let (θ, γ) be as in Theorem 1. Then in the coordinates $(\zeta_1, \zeta_2) = (\theta, \frac{1}{2}\gamma^2)$, the Poincaré return map of the hybrid zero dynamics, $\rho : S \cap Z \to S \cap Z$, is given by

$$\rho(\zeta_2^-) = \delta_{\text{zero}}^2 \, \zeta_2^- - V_{\text{zero}}(\theta^-), \tag{53}$$

with domain of definition

$$\left\{ \zeta_2^- > 0 \mid \delta_{\text{zero}}^2 \, \zeta_2^- - K \geq 0 \right\}. \tag{54}$$

If $\delta_{\text{zero}}^2 \neq 1$ and

$$\zeta_2^* := -\frac{V_{\text{zero}}(\theta^-)}{1 - \delta_{\text{zero}}^2} \tag{55}$$

is in the domain of definition of ρ, then it is the fixed point of ρ. Moreover, if ζ_2^* is a fixed point, then ζ_2^* is an exponentially stable equilibrium point of

$$\zeta_2(k+1) = \rho(\zeta_2(k)) \tag{56}$$

if, and only if, $0 < \delta_{\text{zero}}^2 < 1$, and in this case, its domain of attraction is (54), the entire domain of definition of ρ. □

Proof: This follows directly from the above results. □

These stability results can be reformulated in the following way:

Corollary 1: a) There exists a non-trivial periodic orbit of the hybrid zero dynamics if, and only if, $\delta_{\text{zero}}^2 \neq 1$ and

$$\frac{\delta_{\text{zero}}^2}{1 - \delta_{\text{zero}}^2} V_{\text{zero}}(\theta^-) + K < 0. \tag{57}$$

b) There exists an exponentially stable periodic orbit of the hybrid zero dynamics if, and only if, (57) holds and

$$0 < \delta_{\text{zero}}^2 < 1. \tag{58}$$

---

[1]In general, V_{zero} must be computed numerically.
[2]By definition, $\zeta_2 := \frac{1}{2}(\xi_2)^2$ must be positive along any solution.

□

Remark 3: The Lagrangian of the zero dynamics (28)–(29) can be shown to be $L_{\text{zero}} := K_{\text{zero}} - V_{\text{zero}}$, where V_{zero} is given by (48) and

$$K_{\text{zero}} = \frac{1}{2}\left(\frac{\dot{\xi}_1}{\kappa_1(\xi_1)}\right)^2. \qquad (59)$$

The interpretation of this result will be presented elsewhere. ◁

B. Imposing modeling hypotheses on the zero dynamics

While the domain of definition of the Poincaré map is given in (54), not all solutions of the zero dynamics satisfy the modeling hypotheses; in particular, walking hypothesis GH2 limits the ratio and sign of the ground reaction forces of the stance leg end during phases of single support. This limit is reflected as an upper bound on the domain of definition of ρ. Let F_1^T and F_1^N be the tangential and normal forces experienced at the end of the stance leg. The upper bound will be the largest ζ_2^- such that at some point during the associated phase of single support either F_1^N becomes negative, or $|F_1^T/F_1^N|$ exceeds the maximum allowed static Coulomb friction coefficient.

Calculation of F_1^T and F_1^N requires the full $(N+2)$-DOF model. Consider the model (4) and apply the feedback u^* from (17). Let $\dot{x}_e = f_e(x_e) + g_e(x_e)(F_1^T, F_1^N)'$ be the resulting closed-loop system written in state space form, where, $x_e := (q_e', \dot{q}_e')'$ and $y_e = h_e(q_e) := (p_1^h(q_e), p_1^v(q_e))'$ is the 2-vector of outputs corresponding to the position of the end of the stance leg. It is easily checked that the decoupling matrix $L_{g_e}L_{f_e}h_e$ is invertible, and thus the forces F_1^T and F_1^N may be calculated as

$$\begin{bmatrix} F_1^T \\ F_1^N \end{bmatrix} = -(L_{g_e}L_{f_e}h_e)^{-1}L_{f_e}^2 h_e. \qquad (60)$$

The above expression is quadratic in $\dot{q}_e$, and, when restricted to Z, is affine in ζ_2. Combining this with (47) results in an expression for the forces over a step of the robot that depends only on ξ_1 and ζ_2^-. Express this as

$$\begin{bmatrix} F_1^N(\xi_1, \zeta_2^-) \\ F_1^T(\xi_1, \zeta_2^-) \end{bmatrix} = \Lambda_1(\xi_1)\,\zeta_2^- + \Lambda_0(\xi_1), \qquad (61)$$

where Λ_0 and Λ_1 are smooth functions of ξ_1. Thus, an upper bound on ζ_2^- so that the pivot assumption holds is given by

$$\zeta_{2,F_1^N}^{\max} := \sup_{\zeta_2^-}\left[\min_{\theta^+ \le \xi_1 \le \theta^-} F_1^N(\xi_1, \zeta_2^-)\right] \ge 0 \qquad (62)$$

$$\zeta_{2,|F_1^T/F_1^N|}^{\max} := \sup_{\zeta_2^- \le \zeta_{2,F_1^N}^{\max}}\left[\max_{\theta^+ \le \xi_1 \le \theta^-}\left|\frac{F_1^T(\xi_1, \zeta_2^-)}{F_1^N(\xi_1, \zeta_2^-)}\right|\right] \le \mu_s, \qquad (63)$$

where μ_s is the static Coulomb friction coefficient of the walking surface [30], and the domain of definition of the Poincaré return map should thus be restricted to

$$\left\{\zeta_2^- > 0 \;\middle|\; \delta_{\text{zero}}^2\,\zeta_2^- - K \ge 0,\; \zeta_2^- \le \zeta_{2,|F_1^T/F_1^N|}^{\max}\right\}. \qquad (64)$$

On a practical note, if the modeling hypotheses included bounds on the maximum actuator torque, these bounds could also be explicitly included in the domain of definition of the Poincaré map in the same manner.

C. Creating exponentially stable, periodic orbits in the full model

Fixed points of the Poincaré return map of the hybrid zero dynamics correspond to periodic orbits of the hybrid zero dynamics. By construction of the hybrid zero dynamics, these are also periodic orbits of the full model, (13). Moreover, *exponentially stable orbits* of the hybrid zero dynamics correspond to *exponentially stabilizable orbits* of the full model. This is developed next.

Suppose that hypotheses HH1–HH5 hold and that, in addition, there exists a fixed point, $z^* \in S \cap Z$, of the Poincaré return map for the hybrid zero dynamics. Let $\mathcal{O}$ be the periodic orbit in Z corresponding to z^*; that is,

$$\mathcal{O} := \{z \in Z \mid z = \varphi(t, \Delta(z^*)),\ 0 \le t < T_I \circ \Delta(z^*)\}, \qquad (65)$$

where φ is a solution of the hybrid zero dynamics, (37). $\mathcal{O}$ is then a periodic orbit of the full model corresponding to initial condition z^* and control input $u(t) = u^* \circ \varphi(t, \Delta(z^*))$, for $0 \le t < T_I \circ \Delta(z^*)$, where u^* is given by (17).

The application of the pre-feedback

$$u(x) = (L_g L_f h(x))^{-1}(v - L_f^2 h(x)) \qquad (66)$$

to (3) with an output satisfying HH1–HH4 results in the chain of $N-1$ double integrators,

$$\frac{d^2 y}{dt^2} = v; \qquad (67)$$

see (16). Let $v(y, \dot{y})$ be any feedback controller on (67) satisfying conditions CH2–CH5 of [24], that is,
Controller Hypotheses: for the closed-loop chain of double integrators, $\ddot{y} = v(y, \dot{y})$,
CH2) solutions globally exist on $\mathbb{R}^{2N-2}$, and are unique;
CH3) solutions depend continuously on the initial conditions;
CH4) the origin is globally asymptotically stable, and convergence is achieved in finite time;
CH5) the settling time function[3], $T_{\text{set}} : \mathbb{R}^{2N-2} \to \mathbb{R}$ by

$$\begin{aligned} T_{\text{set}}(y_0, \dot{y}_0) &:= \inf\{t > 0 \mid (y(t), \dot{y}(t)) = (0,0), \\ &\qquad (y(0), \dot{y}(0)) = (y_0, \dot{y}_0)\} \end{aligned}$$

depends continuously on the initial condition, $(y_0, \dot{y}_0)$.
Hypotheses CH2–CH4 correspond to the definition of finite-time stability [7, 25]; CH5 is also needed, but is not implied by CH2–CH4 [8]. These requirements rule out traditional sliding mode control, with its well-known discontinuous action.

Consider now the full-model (13) in closed loop with the feedback

$$u(x) = (L_g L_f h(x))^{-1}(v(h(x), L_f h(x)) - L_f^2 h(x)). \qquad (68)$$

---

[3]That is, the time it takes for a solution initialized at $(y_0, \dot{y}_0)$ to converge to the origin. The terminology is taken from [7].

Take the Poincaré section as S, the walking surface, and let $P : S \rightarrow S$ be Poincaré return map. A simple computation shows that the invariance condition, $\Delta(S \cap Z) \subset Z$, implies that P has a well-defined restriction to $S \cap Z$, and that $P|_{S \cap Z} = \rho$, the Poincaré return map of the hybrid zero dynamics. By Theorem 2 of [24], it therefore follows that $\mathcal{O}$ is exponentially stable for the full model (13) under the feedback (68) if, and only if, it is exponentially stable for the hybrid zero dynamics.

Hence, if an output can be selected so that the resulting 1-DOF hybrid zero dynamics admits an exponentially stable orbit, then an exponentially stable walking motion can be achieved under feedback control for the full dynamical model of the robot. Moreover, by the results of Section IV-B, it can be assured that key modeling assumptions are met for the steady state walking motion. The next parts of the paper look at a means of systematically selecting the output function.

V. COMPUTING AND PARAMETERIZING THE HYBRID ZERO DYNAMICS

The previous section has provided the conditions for the existence of a zero dynamics for the complete robot model with impacts, and established a number of its properties. However, in a concrete manner, the results are not yet practicable for feedback design because the explicit computation of the zero dynamics involves the inversion of a coordinate transformation. This section has two principal objectives. The first is to present a class of output functions that leads to computable, closed-form representations of the zero dynamics. The second objective is to introduce a finite parameterization of the outputs in a convenient form that will permit the shaping of the zero dynamics by parameter optimization.

A. An almost linear output function structure

Consider the following output function

$$y = h(q) := h_0(q) - h_d \circ \theta(q) \tag{69}$$

where $h_0(q)$ specifies $(N-1)$ independent quantities that are to be controlled and $h_d \circ \theta(q)$ specifies the desired evolution of these quantities as a function of the monotonic quantity $\theta(q)$. Driving y to zero will force $h_0(q)$ to track $h_d \circ \theta(q)$. Intuitively, the posture of the robot is being controlled as a holonomic constraint parameterized by $\theta(q)$.

Choosing

$$h_0(q) := H_0 q \tag{70}$$
$$\theta(q) := c\, q \tag{71}$$

where $H_0 : I\!R^N \rightarrow I\!R^{N-1}$ is a linear map, $c : I\!R^N \rightarrow I\!R$ is a linear functional allows the hypotheses of Lemma 1 to be easily satisfied. Concerning those hypotheses, the output function structure (69) with $h_0(q)$ and $\theta(q)$ as in (70) and (71), respectively, satisfies HH1 (the output only depends on the configuration variables) and will satisfy HH3 (invertibility) if, and only if, $H := [H_0'\ c]'$ is full rank. Hence, if HH2 and HH4 hold, the swing phase zero dynamics can be computed in closed form. Indeed, the coordinate inverse

required in (26) is given by

$$q = H^{-1} \left[\begin{array}{c} h_d(\xi_1) \\ \xi_1 \end{array} \right]. \tag{72}$$

In the next section h_d will be specialized to a vector of Bézier polynomials which will make it easy to achieve the invariance condition, $\Delta(S \cap Z) \subset S$.

B. Specialization of h_d by Bézier polynomials

A one-dimensional Bézier polynomial [6] of degree M is a polynomial, $b_i : [0, 1] \rightarrow I\!R$, defined by $M+1$ coefficients, α_k^i, per

$$b_i(s) := \sum_{k=0}^{M} \alpha_k^i \frac{M!}{k!(M-k)!} s^k (1-s)^{M-k}. \tag{73}$$

Some particularly useful features of Bézier polynomials are (see [50, page 291])
1. the image of the Bézier polynomial is contained in the convex hull of the $M + 1$ coefficients (as viewed as points in $I\!R^2$, $\{(0, \alpha_0^i),\ (1/M, \alpha_1^i),\ (2/M, \alpha_2^i), \ldots, (1, \alpha_M^i)\}$) (the polynomial does not exhibit large oscillations with small parameter variations);
2. $b_i(0) = \alpha_0^i$ and $b_i(1) = \alpha_M^i$; and
3. $(\partial b_i(s)/\partial s)|_{s=0} = M\left(\alpha_1^i - \alpha_0^i\right)$ and $(\partial b_i(s)/\partial s)|_{s=1} = M\left(\alpha_M^i - \alpha_{M-1}^i\right)$.
The first feature will be useful for numerical calculations (such as approximating the gradient of a cost function) where numerical stability is crucial. The second two features are exactly those used to achieve $\Delta(S \cap Z) \subset S$.

A given function $\theta(q)$ of the generalized coordinates will not, in general, take values in the unit interval over a phase of single support. Therefore, to appropriately compose a Bézier polynomial with $\theta(q)$, it is necessary to normalize θ by

$$s(q) := \frac{\theta(q) - \theta^+}{\theta^- - \theta^+}, \tag{74}$$

which takes values in $[0, 1]$. Define $h_d \circ \theta(q)$ as

$$h_d \circ \theta(q) := \left[\begin{array}{c} b_1 \circ s(q) \\ b_2 \circ s(q) \\ \vdots \\ b_{N-1} \circ s(q) \end{array} \right]. \tag{75}$$

Group the parameters α_k^i into an $(N-1) \times (M+1)$ matrix, α, and denote the columns of α by $\alpha_k := (\alpha_k^1, \ldots, \alpha_k^{N-1})'$. Evaluating (75) and its derivative with respect to θ at the beginning (resp. end) of a phase of single support, that is, where $\theta(q) = \theta^+$ (resp. $\theta(q) = \theta^-$), leads to the following result.

Theorem 4: (Achieving $\Delta(S \cap Z) \subset Z$) Assume the hypotheses of Theorem 2 and an output h of the form (69) with h_0, h_d, and θ as in (70), (75), and (71), respectively. Then, $h \circ \Delta(S \cap Z) = 0$ if, and only if,

$$\left[\begin{array}{c} \alpha_0 \\ \theta^+ \end{array} \right] = HRH^{-1} \left[\begin{array}{c} \alpha_M \\ \theta^- \end{array} \right]. \tag{76}$$

Moreover, if $\delta_{zero} \neq 0$, then $L_f h \circ \Delta(S \cap Z) = 0$ if, and only if,

$$\alpha_1 = \frac{\theta^- - \theta^+}{Mc\dot{q}^+} H_0 \dot{q}^+ + \alpha_0 \qquad (77)$$

where $\dot{q}^- = \sigma_{\dot{q}}(q_0^-)$ and $\dot{q}^+ := \Delta_{\dot{q}}(q_0^-) \dot{q}^-$. That is, if (76) and (77) hold, then $\Delta(S \cap Z) \subset Z$. $\qquad \square$

Proof: Using Theorem 2 it suffices to show that there exists at least one point $(q_0^-, \dot{q}_0^-) \in S \cap Z$ such that $\gamma_0(q_0^-) \dot{q}_0^- \neq 0$, $h \circ \Delta_q(q_0^-) = 0$, and $L_f h \circ \Delta(q_0^-, \dot{q}_0^-) = 0$. Evaluating (72) on $S \cap Z$, $h \circ \Delta(x^-) = 0$ means that $q|_{\xi_1 = \theta^+} = \Delta_q q|_{\xi_1 = \theta^-}$. This implies

$$H^{-1} \begin{bmatrix} \alpha_0 \\ \theta^+ \end{bmatrix} = R H^{-1} \begin{bmatrix} \alpha_M \\ \theta^- \end{bmatrix}, \qquad (78)$$

which may be solved for $(\alpha_0', \theta^+)'$. Achieving $L_f h \circ \Delta(x^-) = 0$ means that $\dot{q}^+$ must fall in the null space of $\partial h(q)/\partial q$. This can be achieved by choosing α_1 such that

$$\left. \frac{\partial h(q)}{\partial q} \right|_{q=q^+} \dot{q}^+ = \left[H_0 - \frac{M}{\theta^- - \theta^+} (\alpha_1 - \alpha_0) c \right] \dot{q}^+ = 0. \qquad (79)$$

Since $\gamma_0(q_0^-) \dot{q}_0^- \neq 0$ by assumption it follows[4] that $c\dot{q}^+ \neq 0$ and the solvability of (79) for α_1 is ensured. $\qquad \square$

Remark 4: Theorem 4 constrains the coefficients α_0 and α_1 to be functions of α_M. Hence, M must be chosen to be three or greater to impose configuration and velocity periodicity. $\qquad \triangleleft$

VI. Creating Exponentially Stable Fixed Points Through Optimization

The use of optimization in the analysis and design of biped walking motions is not a new concept. Work as early as the 1970's can be found in the biomechanics literature (see [17, 28], for example). In more recent years, the design of optimal or approximately optimal trajectories for biped robots has become a popular topic [12, 14, 16, 26, 27, 52, 53, 55]. In each case the approach has been to design time trajectories such that a defined cost is minimized, or approximately minimized, subject to a set of constraints. The optimization technique employed varies. Cabodevila and Abba [12] parameterized the robot state as a finite Fourier series and compared the performance of three algorithms: Nelder and Mead, Genetic, and Simulated Annealing. Chevallereau and Aoustin [14], and Chevallereau and Sardain [16] rewrote the actuated dynamics of the robot as a polynomial function of the unactuated dynamics and used Sequential Quadratic Programming (SQP). Hasegawa, Arakawa, and Fukuda [27] used a modified genetic algorithm to generate reference trajectories parameterized as cubic splines. Hardt [26] used

---

[4]First note that $\xi^+ = \delta_{zero}\xi^- \neq 0$ where $\xi^- = \gamma_0(q_0^-)\dot{q}_0^-$ since $\delta_{zero} \neq 0$ and $\xi^- \neq 0$ by assumption. Next note that since both $(\xi_1, L_f\xi_1)$ and (ξ_1, ξ_2) are valid coordinates on Z the coordinate transformation $\Xi : (\xi_1, \xi_2) \to (\xi_1, L_f\xi_1)$, $\Xi = (\xi_1, \kappa_1(\xi_1)\xi_2)$, is a full rank map. This implies $\kappa_1(\xi_1) \neq 0$ since

$$\frac{\partial \Xi}{\partial(\xi_1, \xi_2)} = \begin{bmatrix} 1 & 0 \\ \star & \kappa_1(\xi_1) \end{bmatrix}.$$

Hence, $\xi_2 \neq 0$ implies $L_f\xi_1 = c\dot{q} \neq 0$.

an optimization package, DIRCOL [62], which implements a sparse SQP algorithm and uses a variable number of cubic splines to approximate the state and piecewise linear functions to approximate the control signals. Rostami and Bessonnet [53] applied Pontryagin's Maximum Principle. Roussel, Canudas-de-Wit, and Goswami [55] approximated the dynamics and used a direct shooting optimization algorithm. While the approach presented here uses the same optimization algorithm as in [26], the result of the optimization is not an optimal or approximately optimal open-loop trajectory, but rather a *closed-loop system* which creates an exponentially stable orbit, and along this orbit energy consumption has been approximately minimized while satisfying other natural kinematic and dynamic constraints.

Consider the system (13) with output (69) with h_0, h_d, and θ as in (70), (75), and (71), respectively. Choosing the parameters of (70), (75), and (71) to satisfy the assumptions of Theorem 4 guarantees that the hybrid zero dynamics exist and the unique control associated with the single support phase of model (13) is given by (17). The goal of the approximate optimization will be to minimize an appropriate cost function while simultaneously satisfying a number of constraints.

Consider the hybrid zero dynamics (37) with cost function

$$J(\alpha) := \frac{1}{p_2^h(q_0^-)} \int_0^{T_I(\xi_2^-)} \sum_{i=1}^{N-1} (u_i^*(t))^2 dt, \qquad (80)$$

where $T_I(\xi_2^-)$ is the step duration, $p_2^h(q_0^-)$ corresponds to step length, and $u^*(t)$ is the result of evaluating (17) along a solution of the hybrid zero dynamics. It is interesting to note that $T_I(\xi_2^-)$ may be calculated from (28) as

$$T_I(\xi_2^-) = \int_{\theta^+}^{\theta^-} \frac{1}{\kappa_1(\xi_1)\xi_2(\xi_1, \xi_2^-)} d\xi_1 \qquad (81)$$

where $\xi_2(\xi_1, \xi_2^-)$ is a solution of (46) and is monotonic in ξ_2^- which implies that $T_I(\xi_2^-)$ is monotonic in ξ_2^-.

The total number of parameters for optimization is $(N-1)(M-1)$; $M-1$ free parameters for each output[5]. The optimization problem may be expressed in Mayer form [4, page 332] as

$$\dot{x}_1 = \kappa_1(x_1) x_2 \qquad (82)$$
$$\dot{x}_2 = \kappa_2(x_1) \qquad (83)$$
$$\dot{x}_3 = \sum_{i=1}^{N-1} (u_i^*(x_1, x_2))^2. \qquad (84)$$

The constraints may be divided into three classes: nonlinear inequality constraints (NIC's), nonlinear boundary equality constraints (NBEC's), and explicit boundary constraints (EBC's). The NIC's must be satisfied at each point in the time interval of optimization; the NBEC's only need to be satisfied at the beginning or end of the time interval of optimization; and the EBC's give the initial or final state. The following constraints are typically required:

---

[5]By Theorem 4 two parameters per output can be calculated from the other $M-1$.

Nonlinear Inequality Constraints: The following three NIC's enforce modeling assumptions per constraints on

NIC1) minimum normal ground reaction force experienced by the stance leg end;

NIC2) maximum ratio of tangential to normal ground reaction forces experienced by the stance leg end; and

NIC3) swing leg end height to ensure S intersects Z only the end of the step.

Note that other NIC's, such as a constraint on minimum hip height, are in general required to achieve a desired walking style.

Nonlinear Boundary Equality Constraints: There are five natural NBEC's that enforce

NBEC1) the average forward walking rate, $\bar{\nu}$, defined as step length divided by step duration

$$\bar{\nu} := \frac{p_2^h(q_0^-)}{T_I(\xi_2^-)}; \qquad (85)$$

NBEC2) that the post-impact velocity of the swing leg is positive;

NBEC3) the validity of the impact of the swing leg end with the walking surface;

NBEC4) the existence of a fixed point, $\zeta_2^* > K/\delta_{\text{zero}}^2$; and

NBEC5) the stability of the fixed point, $0 < \delta_{\text{zero}}^2 < 1$.

Explicit Boundary Constraints: There are five EBC's that give the state at $t = 0$ and $t = T_I(\xi_2^-)$,

EBC1) $x_1(0) = c\,\Delta_q\,\sigma_q$;

EBC2) $x_2(0) = \gamma \circ \Delta \circ \sigma(\zeta_2^*)$;

EBC3) $x_3(0) = 0$;

EBC4) $x_1(T_I(\xi_2^-)) = c\,\sigma_q$; and

EBC5) $x_2(T_I(\xi_2^-)) = \gamma \circ \sigma(\zeta_2^*)$.

Note that $x_3(T_I(\xi_2^-))$ cannot be explicitly given as its calculation requires knowledge of x_1 and x_2 over the entire time interval of optimization.

Note that without use of the hybrid zero dynamics there would be $2N$ states, the derivative of the cost, and $N-1$ control signals to be included in the problem formulation, while stability of the closed-loop system would be hard to quantify and include as a simple optimization constraint. After optimization, hypothesis HH2, the invertibility of the decoupling matrix, must be checked. This condition is essentially guaranteed whenever $J(\alpha)$ is finite, since singularities in $L_g L_f h$ will normally result in u^* taking on unbounded values; however, a simply connected, open set about the periodic orbit where the decoupling matrix is invertible can be *explicitly* computed by a method developed in [45].

VII. Example: 5-Link Biped Walker

The goal of this section is to illustrate the application of the presented framework for stability analysis and performance enhancement. This will be done on the 5-link biped robot depicted in Figure 2 which satisfies hypotheses RH1–RH5. For this robot GH1–GH6 will be satisfied by restricting choice of walking gaits appropriately during the optimization process.

A. Robot model

The 5-link model corresponds to the model of a prototype 5-link biped called RABBIT, which is under construction by the French project *Commande de Robots à Pattes* of the *CNRS - GdR Automatique* [1]. Table I gives the model parameters. Figures 4 and 5 detail the measurement conventions. The equations of motion as well as particulars of the impact model are omitted here for reasons of space but can be found at [2] in various printable formats.

B. Almost linear output function choice

Choosing $H_0 = [I, \ 0]$ and $c = (-1, \ 0, \ -1/2, \ 0, \ -1)$ clearly guarantees that H is invertible and results in the output

$$y = h_0(q) - h_d \circ \theta(q) = \begin{bmatrix} q_{31} \\ q_{32} \\ q_{41} \\ q_{42} \end{bmatrix} - h_d \circ \theta(q). \qquad (86)$$

In light of Remark 4, M is chosen to be 6 which leaves five free parameters to be chosen for each output. This implies a total of 20 output function parameters to be optimized.

For particular choice of α, HH4 must be checked to ensure smoothness of $S \cap Z$. This entails evaluating the rank[6] of

$$\frac{\partial}{\partial q} \begin{bmatrix} h(q) \\ p_2^v(q) \end{bmatrix} \Bigg|_{x \in S \cap Z} = \begin{bmatrix} H_0 - \frac{M}{\theta^- - \theta^+}\,(\alpha_M - \alpha_{M-1})\,c \\ \frac{\partial p_2^v(q)}{\partial q}\Big|_{q=q_0^-} \end{bmatrix}. \qquad (87)$$

where $p_2^v(q)$ is the height of the swing end. Hypothesis HH2, the invertibility of the decoupling matrix, is checked for choice of α by using the technique presented in [45]. If the optimization constraints are satisfied, as detailed in Section VI, so will the remaining gait, impact model, and output function hypotheses.

C. Parameter choice via approximate optimization

Three additional NIC's are required for the example robot model to walk with a human-like gait. The first two, when satisfied, prevent the stance and swing leg knees from hyper-extending. The third, when satisfied, prevents the hips from dropping too low.

The optimization package DIRCOL was used to solve the optimization problem. The implementation was straightforward with the exception that DIRCOL is unable to handle non-constant initial EBC's. For this reason EBC1 and EBC2 must be converted into NBEC's[7].

Table II summarizes the result of optimizing for a desired average forward walking rate of 1.05 m/s. The optimization took 1240 sec (≈ 21 min) on a PC based computer with a 1 GHz Pentium III processor. The walking motion is exponentially stable since $0 < \delta_{\text{zero}}^2 < 1$ and $\zeta_2^* > K/\delta_{\text{zero}}^2 = 408.2$. Figure 6 is a stick figure animation of this result for a single step. The walking motion appears to be natural. Figure 7 is a plot of the associated torques at the fixed point. Of the four associated torques, the peak

---

[6]See Remark 1.

[7]This is accomplished for EBC1 by the construction

$$\mathrm{NBEC}_{\mathrm{EBC1}} = \begin{cases} 0, & x_1(0) - c\,\Delta_q\,\sigma_q = 0 \\ |x_1(0) - c\,\Delta_q\,\sigma_q|, & \text{otherwise} \end{cases}$$

and similarly for EBC2.

torque occurs at the stance leg hip and is approximately $47\ Nm$. Note that this is comparable to the torques associated with walking at $0.75\ m/s$ as determined in [14]. The peak power is also associated with the stance leg hip and is approximately $267\ W$. Figure 9 gives κ_1 and κ_2 as functions of ξ_1. Notice that κ_1 is strictly positive while κ_2 is sign-indefinite. Movies of the walking motion may be found at [2].

VIII. Conclusion

The notion of the hybrid zero dynamics has been introduced for a one degree of underactuation, planar, bipedal walker with rigid impacts. This two-dimensional, invariant sub-dynamics of the complete hybrid model of the biped robot was shown to be key to designing exponentially stabilizing controllers for walking motions. In particular, exponentially stable orbits of the hybrid zero dynamics can be rendered exponentially stable in the complete hybrid model. Since the Poincaré map of the hybrid zero dynamics is diffeomorphic to a scalar, LTI system, the existence and stability properties of orbits of the hybrid zero dynamics are particularly easy to characterize. It was shown how a special class of output functions can be used to simplify the actual computation of the hybrid zero dynamics, while at the same time inducing a convenient, finite parameterization of the hybrid zero dynamics. Parameter optimization was then applied to the hybrid zero dynamics to directly design a provably stable, closed-loop system with satisfied design constraints, such as walking at a given average speed and the forces on the support leg lying in the allowed friction cone. All of the results were illustrated on a five-link walker.

The key property permitting the above analysis is the invariance of the swing-phase zero dynamics under the impact map, thereby creating a two-dimensional invariant surface in the full hybrid model. Without this property, a "stability" analysis of the swing-phase zero dynamics makes no sense. In [39], invariance of the swing-phase zero dynamics was achieved only at a point, thereby creating a one-dimensional invariant surface (i.e., a periodic orbit) in the full order model. In [24], an even weaker form of invariance was achieved: the swing-phase zero dynamics became invariant under the impact map only in the limit under high-gain feedback control. In work to be published, it will be shown that the framework of the hybrid zero dynamics also allows the design of transition controllers for switching with stability among controllers that achieve stable walking at discrete speeds, and for achieving walking at a continuum of speeds [63].

Acknowledgments

References

[1] http://www-lag.ensieg.inpg.fr/prc-bipedes/english/.

[2] http://www.eecs.umich.edu/~grizzle/papers/robotics.html .

[3] V. I. Babitsky. *Theory of Vibro-Impact Systems and Applications*. Foundations of Engineering Mechanics. Springer, Berlin, 1998.

[4] S.P. Banks. *Control systems engineering*. Prentice Hall, Englewood Cliffs, 1986.

[5] M.D. Berkemeier and R.S. Fearing. Tracking fast inverted trajectories of the underactuated acrobot. *IEEE Transactions on Robotics and Automation*, 15(4):740–750, August 1999.

[6] P. Bézier. *Numerical Control: Mathematics and Applications*. John Wiley & Sons, New York, 1972.

[7] S.P. Bhat and D.S. Bernstein. Continuous finite-time stabilization of the translational and rotational double integrators. *IEEE Transactions on Automatic Control*, 43(5):678–682, 1998.

[8] S.P. Bhat and D.S. Bernstein. Finite-time stability of continuous autonomous systems. *Preprint*, 1998.

[9] W.M. Boothby. *An Introduction to Differentiable Manifolds and Riemannian Geometry*. Academic Press, New York, 1975.

[10] B. Brogliato. *Nonsmooth Impact Dynamics: Models, Dynamics and Control*, volume 220 of *Lecture Notes in Control and Information Sciences*. Springer, London, 1996.

[11] M. Bühler, D. E. Koditschek, and P.J. Kindlmann. A family of robot control strategies for intermittent dynamical environments. *IEEE Control Systems Magazine*, 10(2):16–22, Feb 1990.

[12] G. Cabodevilla and G. Abba. Quasi optimal gait for a biped robot using genetic algorithm. In *Proc. of the IEEE International Conference on Systems, Man and Cybernetics, Computational Cybernetics and Simulationms, Orlando, FL*, pages 3960–3965, October 1997.

[13] C. Chevallereau. Parameterized control for an underactuated biped robot. In *IFAC 2002, Barcelona, Spain*, July 2002.

[14] C. Chevallereau and Y. Aoustin. Optimal reference trajectories for walking and running of a biped robot. *Robotica*, 19(5):557–569, September 2001.

[15] C. Chevallereau, A. Formal'sky, and B. Perrin. Control of a walking robot with feet following a reference trajectory derived from ballistic motion. In *Proc. of the IEEE International Conference on Robotics and Automation, Albuquerque, N.M.*, pages 1094–1099, April 1997.

[16] C. Chevallereau and P. Sardain. Design and actuation optimization of a 4 axes biped robot for walking and running. In *Proc. of the IEEE International Conference on Robotics and Automation, San Francisco, California*, pages 3365–3370, April 2000.

[17] C.K. Chow and D.H. Jacobson. Studies of human locomotion via optimal programming. *Mathematical Biosciences*, 10:239–306, 1971.

[18] M. Conditt and F. Mussa-Ivaldi. Central representation of time during motor learning. *Proceedings of the National Academy of Sciences of the United States of America*, 96:11625–11630, September 1999.

[19] J.J. Craig. *Introduction to robotics: mechanics and control*. Addison-Wesley, Reading, MA, 1989.

[20] B. Espiau and A. Goswani. Compass gait revisited. In *Proc. of the IFAC Symposium on Robot Control, Capri, Italy*, pages 839–846, September 1994.

[21] R. Full and D. Koditschek. Templates and anchors: Neuromechanical hypotheses of legged locomotion on land. *Journal of Experimental Biology*, 202:3325–3332, December 1999.

[22] A. Goswani, B. Espiau, and A. Keramane. Limit cycles and their stability in a passive bipedal gait. In *Proc. of the IEEE International Conference on Robotics and Automation, Minneapolis, MN.*, pages 246–251, April 1996.

[23] J.W. Grizzle, G. Abba, and F. Plestan. Proving asymptotic stability of a walking cycle for a five dof biped robot model. In *2nd Int. Conf. on Climbing and Walking Robots, CLAWAR-99, Portsmouth, U.K.*, pages 69–81, September 1999.

[24] J.W. Grizzle, G. Abba, and F. Plestan. Asymptotically stable walking for biped robots: Analysis via systems with impulse effects. *IEEE Transactions on Automatic Control*, 46:51–64, January 2001.

[25] V.T. Haimo. Finite time controllers. *SIAM J. Control and Optimization*, 24(4):760–770, 1986.

[26] M.W. Hardt. *Multibody dynamical Algorithms, Numerical Optimal Control, with Detailed Studies in the Control of Jet Engine Compressors and Biped Walking*. PhD thesis, University of California, San Diego, 1999.

[27] Y. Hasegawa, T. Arakawa, and T. Fukuda. Trajectory generation for biped locomotion. *Mechatronics*, 10(1–2):67–89, March 2000.

[28] H. Hatze. The complete optimization of a human motion. *Mathematical Biosciences*, 28:99–135, 1976.

[29] K. Hirai, M. Hirose, Y. Haikawa, and T. Takenake. The development of honda humanoid robot. In *Proc. of the IEEE International Conference on Robotics and Automation, Leuven, Belgium*, pages 1321–1326, May 1998.

[30] Y. Hurmuzlu and D.B. Marghitu. Rigid body collisions of planar kinematic chains with multiple contact points. *International Journal of Robotics Research*, 13(1):82–92, 1994.

[31] A. Isidori. *Nonlinear Control Systems: An Introduction.* Springer-Verlag, Berlin, third edition, 1995.

[32] A. Isidori and C. Moog. On the nonlinear equivalent of the notion of transmission zeros. In Byrnes C. and A. Kurzhanski, editors, *Proc. of the IIASA Conference: Modeling and Adaptive Control*, pages 146–157, Berlin, 1988. Springer-Verlag.

[33] K. Ito, F. Matsuno, and R. Takahashi. Underactuated crawling robot. In *Proc. of the IEEE International Conference on Intelligent Robotos and Systems, Takamatsu, Japan.*, pages 1684–1689, October–November 2000.

[34] S. Kajita and K. Tani. Experimental study of biped dynamic walking. *IEEE Control Systems Magazine*, 16(1):13–19, February 1996.

[35] R. Katoh and M. Mori. Control method of biped locomotion giving asymptotic stability of trajectory. *Automatica*, 20(4):405–414, 1984.

[36] M. Kawato. Internal models for motor control and trajectory planning. *Current Opinion in Neurobiology*, 9:718–727, 1999.

[37] D.D. Koditschek and M. Buhler. Analysis of a simplified hopping robot. *International Journal of Robotics Research*, 10(6):587–605, 1991.

[38] D. W.. Marhefka and D. Orin. Simulation of contact using a nonlinear damping model. In *Proc. of the IEEE International Conference on Robotics and Automation, Minneapolis, MN.*, pages 1662–1668, April 1996.

[39] T.G. McGee and M.W. Spong. Trajectory planning and control of a novel walking biped. In *IEEE International Conference on Control Applications, Mexico City, Mexico*, pages 1099–1104, September 2001.

[40] R.M. Murray, Z. Li, and S. Sastry. *A Mathematical Introduction to Robotic Manipulation.* CRC Press, Boca Raton, 1993.

[41] J. Nakanishi, T. Fukuda, and D. Koditschek. A brachiating robot controller. *IEEE Transactions on Robotics and Automation*, 16(2):109–123, April 2000.

[42] H. Nijmeijer and van der Schaft,A. J. *Nonlinear Dynamical Control Systems.* Springer-Verlag, Berlin, 1989.

[43] K. Ono, R. Takahashi, A. Imadu, and T. Shimada. Self-excitation control for biped walking mechanism. In *Proc. of the IEEE International Conference on Intelligent Robotos and Systems, Takamatsu, Japan.*, pages 1143–1148, October–November 2000.

[44] K. Ono, K. Yamamoto, and A. Imadu. Control of giant swing motion of a two-link horizontal bar gymnastic robot. *Advanced Robotics*, 15(4):449–465, 2001.

[45] F. Plestan, J.W. Grizzle, E.R. Westervelt, and G. Abba. Stable walking of a 7-dof biped robot. In *Accepted for publication in IEEE Transactions on Robotics and Automation*, February 2001.

[46] J. Pratt, M.C. Chee, A. Torres, P. Dilworth, and G. Pratt. Virtual model control: an intuitive approach for bipedal locomotion. *International Journal of Robotics Research*, 20(2):129–143, February 2001.

[47] J. Pratt and G. Pratt. Intuitive control of a planar bipedal walking robot. In *Proc. of the IEEE International Conference on Robotics and Automation, Leuven, Belgium*, pages 2014–2021, May 1998.

[48] M.H. Raibert, S. Tzafestas, and C. Tzafestas. Comparative simulation study of three control techniques applied to a biped robot. In *Proc. of the IEEE International Conference on Systems, Man and Cybernetics Systems Engineering in the Service of Humans, Le Touquet, France*, pages 494–502, October 1993.

[49] A. Rizzi and D. Koditschek. An active visual estimator for dexterous manipulation. *IEEE Transactions on Robotics and Automation*, 12(5):697–713, October 1996.

[50] D.F. Rogers and J.A. Adams. *Mathematical Elements for Computer Graphics.* McGraw-Hill, New York, second edition, 1990.

[51] J.A. Rosas-Flores, J. Alvarez-Gallegos, and R. Castro-Linares. Stabilization of a class of underactuated systems. In *Proc. IEEE International Conference on Decision and Control, Sydney, Australia*, pages 2168–2173, December 2000.

[52] M. Rostami and G. Bessonnet. Sagittal gait of a biped robot during the single support phase. part 1: passive motion. *Robotica*, 19:163–176, March–April 2001.

[53] M. Rostami and G. Bessonnet. Sagittal gait of a biped robot dur-
ing the single support phase. part 2: optimal motion. *Robotica*, 19:241–253, May–June 2001.

[54] L. Roussel. *Génération de trajectoires de marche optimales pour un robot bipède.* PhD thesis, Institut National Polytechnique - Grenoble - France, November 1998.

[55] L. Roussel, C. Canudas-de Wit, and A. Goswami. Generation of energy optimal complete gait cycles for biped robots. In *Proc. of the IEEE International Conference on Robotics and Automation, Leuven, Belgium*, pages 2036–2041, May 1998.

[56] A. Sano and J. Furusho. Realization of natural dynamic walking using the angular momentum information. In *Proc. of the IEEE International Conference on Robotics and Automation, Cincinnati, OH.*, pages 1476–1481, May 1990.

[57] U. Saranli, W. Schwind, and D. Koditschek. Toward the control of a multi-jointed, monoped runner. In *Proc. of the IEEE International Conference on Robotics and Automation, Leuven, Belgium*, pages 2676–2682, May 1998.

[58] C.L. Shih and W.A. Gruver. Control of a biped robot in the double-support phase. *IEEE Transactions on Systems, Man, and Cybernetics*, 22(4):729–735, 1992.

[59] M.W. Spong. The swing up control problem for the acrobot. *IEEE Control Systems Magazine*, 15(1):49–55, February 1995.

[60] M.W. Spong. Passivity based control of the compass gait biped. In *Proc. of IFAC World Congress, Beijing, China*, July 1999.

[61] M.W. Spong and M. Vidyasagar. *Robot Dynamics and Control.* John Wiley & Sons, New York, 1989.

[62] O. von Stryk. *DIRCOL User's Guide.* Technische Universität Müchen, Zentrum Mathematik (SCB), Lehrstuhl M2 Höhere Mathematik und Numerische Mathematik, D-80290, Müchen, Germany, 2.1 edition, 1999.

[63] E.R. Westervelt, J.W. Grizzle, and C. Canudas de Wit. Switching and PI control of walking motions of planar biped walkers. *Accepted for publication in IEEE Transactions on Automatic Control*, 2002. See [2] for a preprint.

[64] H. Ye, A.N. Michel, and L. Hou. Stability theory for hybrid dynamical systems. *IEEE Transactions on Automatic Control*, 43(4):461–474, April 1998.

APPENDIX

I. PROOF OF PROPOSITION 1

Proof: Without loss of generality, assume $\hat{\theta}(t_0) < \hat{\theta}(t_f)$. Then $\dot{\hat{\theta}}(t_0) > 0$. To show that $\hat{\theta}(t)$ is monotonic it suffices to show that $\dot{\hat{\theta}}(t) > 0$ for all $t_0 < t < t_f$. Suppose there exists some t_2 (see Figure 8) such that $t_0 < t_2 < t_f$ and $\dot{\hat{\theta}}(t_2) = 0$. Let t_2 be the smallest such t. The point $(\hat{\theta}(t_2), 0)$ cannot be an equilibrium point of (22) because $\hat{\theta}(t_2) < \hat{\theta}(t_f)$. Hence, there exits some $t_3 > t_2$ such that for all $t_2 < t < t_3$, $\dot{\hat{\theta}}(t) < 0$ and $\hat{\theta}(t) < \hat{\theta}(t_2)$. By the assumption that $\hat{\theta}(t) > \hat{\theta}(t_0)$ for all $t > t_0$ and because $\hat{\theta}(t_f) > \hat{\theta}(t_2)$, there must exist a $t_4 > t_3$ such that $\hat{\theta}(t_4) = \hat{\theta}(t_1)$ for some $t_0 < t_1 < t_2$. This contradicts the uniqueness of solutions of (22). Hence, there can be no t_2 such that $\dot{\hat{\theta}}(t_2) = 0$ and thus $\dot{\hat{\theta}}(t) > 0$ for all $t_0 < t < t_f$. Therefore, $\hat{\theta} : [t_0, t_f] \to I\!R$ is strictly monotonic. ☐

II. TABLES AND FIGURES

Model parameters	Torso (T)	Femurs (f)	Tibias (t)
Mass, M_* (kg)	20	6.8	3.2
Length, L_* (m)	0.625	0.4	0.4
Inertia, I_* (m^2kg)	2.22	1.08	0.93
Mass Center, p_*^M (m)	0.2	0.163	0.128

TABLE I

MODEL PARAMETERS FOR EXAMPLE ROBOT

$J(\alpha)$ (N^2m)	ζ_2^* $(kgm^2/s)^2$	δ_{zero}^2 -	$V_{\text{zero}}(\theta^-)$ $(kgm^2/s)^2$	K $(kgm^2/s)^2$
36.79	979.0	0.638	−354.4	260.4

TABLE II

OPTIMIZATION RESULT STATISTICS

Fig. 5. Schematic of torso with measurement conventions.

Fig. 6. Stick animation of robot taking one step from left to righ. Note that the stance leg is dotted.
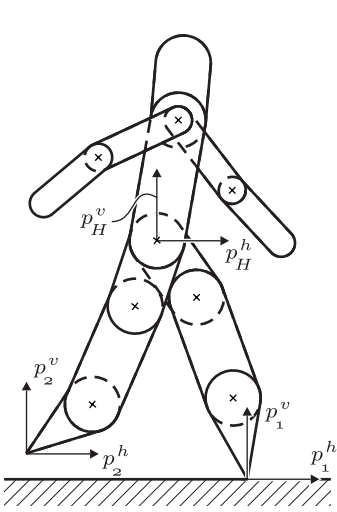
Fig. 1. A higher DOF robot model. Cartesian coordinates are indicated at the hips and the leg ends.
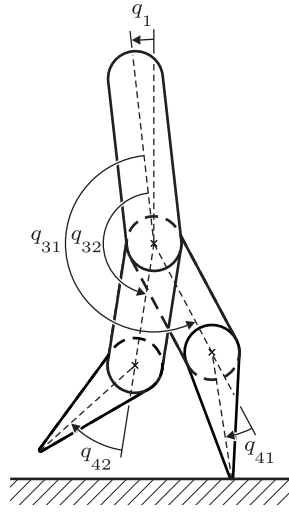
Fig. 2. Schematic of the 5-link robot considered with measurement conventions.

Fig. 7. Torque curves for three steps for the example.
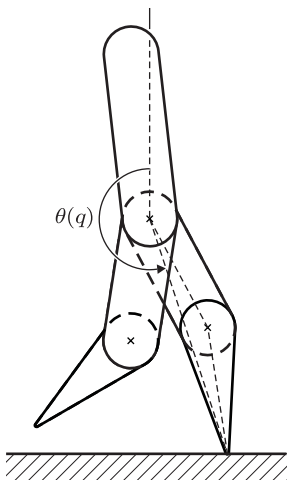
Fig. 3. Example $\theta(q)$ measured between the vertical and the line connecting the hips and the stance leg end.
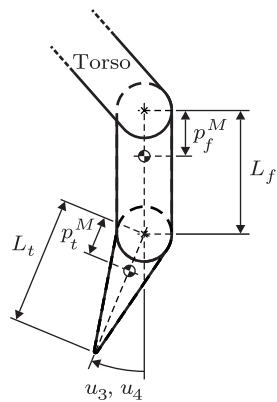
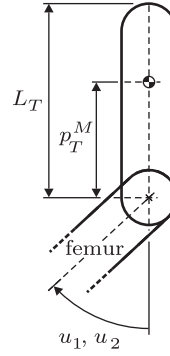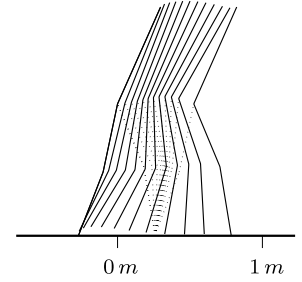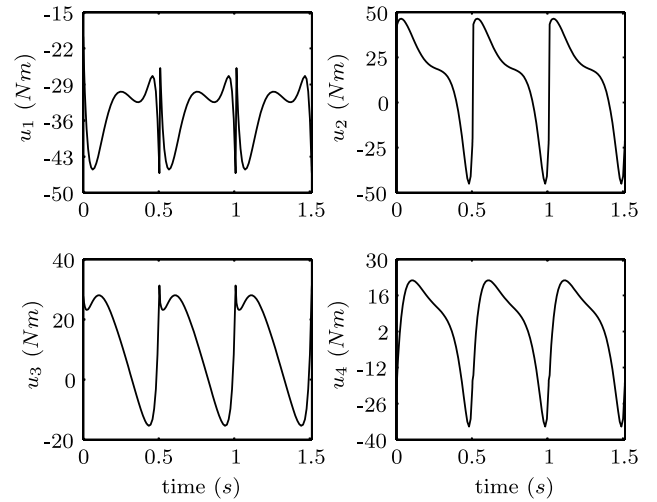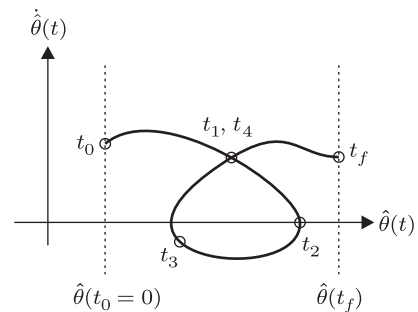Fig. 4. Schematic of leg with measurement conventions.
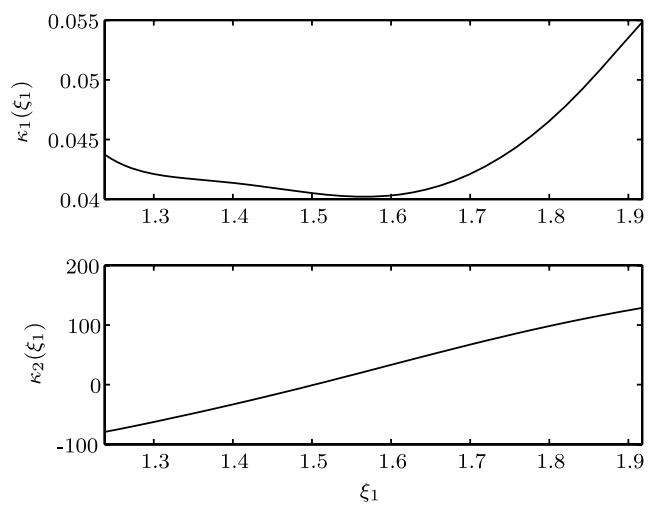
Fig. 8. Impossible integral curve of the zero dynamics.

Fig. 9. Constituent functions of the zero dynamics for the example.